

# 1 Analysis of Energy Flux Vector on Natural Convection 2 Heat Transfer in Porous Wavy-Wall Square Cavity with 3 A Partially-Heated Surface

4 Yan-Ting Lin<sup>1</sup> and Ching-Chang Cho<sup>2\*</sup>

5 <sup>1</sup>Institute of Nuclear Energy Research, Atomic Energy Council, Taiwan

6 <sup>2</sup>Department of Vehicle Engineering, National Formosa University,  
7 No.64, Wunhua Rd., Huwei Township, Yunlin County, Taiwan

8 \* Correspondence: : cccho@nfu.edu.tw; Tel.: +886-5-6315699

9 **Abstract:** The study utilizes the energy-flux-vector method to analyze the heat transfer  
10 characteristics of natural convection in a wavy-wall porous square cavity with a partially-heated  
11 bottom surface. The effects of the modified Darcy number and modified Rayleigh number on the  
12 energy-flux-vector distribution and mean Nusselt number are examined. The results show that  
13 when a low modified Darcy number with any value of modified Rayleigh number is given, the  
14 recirculation regions are not formed in the energy-flux-vector distribution within the porous  
15 cavity. Therefore, a low mean Nusselt number is obtained. The recirculation regions do still not  
16 form and thus the mean Nusselt number has a low value when a low modified Darcy number  
17 with a high modified Rayleigh number is given. However, when the values of the modified Darcy  
18 number and modified Rayleigh number are high, the energy flux vectors generate recirculation  
19 regions and thus a high mean Nusselt number is obtained.

20 **Keywords:** energy-flux-vector; porous cavity; natural convection; wavy-wall  
21

## 22 1. Introduction

23 The plot of the heat energy flow paths is important since it can provide physical insights into  
24 the energy transport process in detail. To achieve this purpose, Kimura and Bejan [1] have  
25 suggested a heatline visualization technique. Following the study of the Kimura and Bejan [1],  
26 numerous researchers have explored the transport process of heat energy within thermal-fluid  
27 systems by utilizing the technique [2-4].

28 Hooman [5, 6] has presented an energy-flux-vector method, which is basically similar to the  
29 heatline technique, for visualizing the transport process of heat energy. Comparing the two  
30 visualization methods, Hooman [5, 6] has pointed out that the energy-flux-vector method is better  
31 than the heatline visualization technique since the algebraic equations do not require to be solved  
32 [5-8]. In the literature, numerous researchers [7-9] have demonstrated that the transport process of  
33 heat energy can be completely explained by using the energy-flux-vector method.

34 Natural convection phenomenon in porous cavities has numerous practical applications in  
35 engineering fields, including biomedical engineering, geothermal engineering, thermal insulation,  
36 solar collection, and so on [10, 11]. To achieve the purpose of heat transfer enhancement,  
37 wavy-surface geometries often imposed [7, 8]. In the literature, the investigation into the natural  
38 convection heat transfer behavior in a porous cavity with wavy surfaces has been widely discussed  
39 [12-14]. The results have demonstrated that the use of the wavy-surface geometries can improve the  
40 heat transfer effect within a porous cavity. Recently, Biswal et al. [15] have utilized the  
41 energy-flux-vector method for explaining the transport process of heat energy of natural convection  
42 within a porous cavity with curved side walls. Their results have shown that given suitable  
43 curved-sidewall forms with appropriate flow conditions, the heat transfer effect can be enhanced.

44 In the current study, the energy-flux-vector method is utilized to analyze the heat transfer  
45 characteristics of natural convection within a porous square cavity bounded by a partially-heated  
46 flat bottom wall, low temperature left and right wavy-walls, and a insulated flat top wall. The

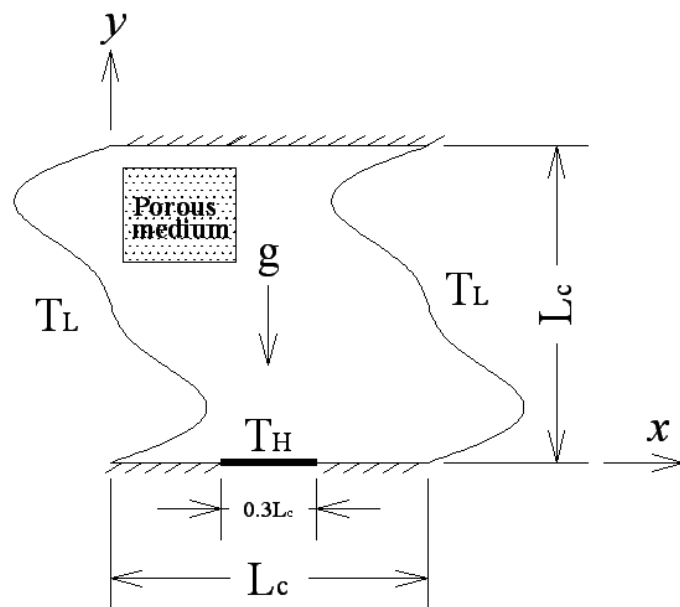
47 simulations focus particularly on the effects of the modified Darcy number and modified Rayleigh  
 48 number on the energy-flux-vector distribution and mean Nusselt number, respectively.

49 **2. Mathematical Formulation**

50 *2.1. Governing Equations and Boundary Conditions*

51 Figure 1 illustrates the studied porous square wavy-wall cavity with a partially-heated bottom  
 52 surface and a characteristic length of  $L_c$ . As shown, the partially-heated wall surface has a length  
 53 of  $0.3L_c$ , and it is placed on the center of the bottom wall. Meanwhile, the left and right walls are  
 54 assumed to have a constant low temperature and a complex-wavy surface.

55 It is assumed that the working fluid is Newtonian, incompressible, and the flow and  
 56 temperature fields are two-dimensional, laminar and steady state. In addition, it is assumed that the  
 57 Boussinesq approximation is imposed, and local thermal equilibrium condition is achieved.



58  
 59 **Figure 1.** Geometry of partially-heated wavy-wall porous cavity.

60 Let the following non-dimensional quantities be introduced [16]:

$$61 \quad x^* = \frac{x}{L_c}, \quad y^* = \frac{y}{L_c}, \quad \alpha_{eff} = \frac{k_{eff}}{\varepsilon \rho C_p}, \quad u^* = \frac{u L_c}{\alpha_{eff}}, \quad v^* = \frac{v L_c}{\alpha_{eff}}, \quad p^* = \frac{p L_c^2}{\rho \alpha_{eff}^2}, \quad \theta = \frac{T - T_L}{T_H - T_L},$$

$$62 \quad K_m = \frac{K}{\varepsilon}, \quad \text{Pr}_m = \frac{\mu}{\rho \alpha_{eff}}, \quad Da_m = \frac{K_m}{L_c^2}, \quad Ra_m = \frac{\rho g \beta L_c^3 (T_H - T_L)}{\mu \alpha_{eff}} \quad (1)$$

63 where  $\alpha_{eff}$  is the effective thermal diffusivity;  $k_{eff}$  is the effective thermal conductivity;  $\varepsilon$  is the  
 64 porosity;  $\rho$  is the density;  $C_p$  is the specific heat;  $u$  and  $v$  are the velocity components along  
 65  $x$ - and  $y$ -axes, respectively;  $p$  is the pressure;  $\theta$  is the dimensionless temperature;  $T$  is the  
 66 temperature;  $T_H$  and  $T_L$  are the high temperature and low temperature, respectively;  $K$  is the  
 67 permeability;  $\text{Pr}_m$  is the modified Prandtl number;  $Da_m$  is the modified Darcy number;  $Ra_m$  is  
 68 the modified Rayleigh number;  $g$  is the gravitational acceleration;  $\beta$  is the thermal expansion  
 69 coefficient; subscripts  $m$  indicates the modified value; and superscript  $*$  denote the  
 70 non-dimensional quantity. After the viscous dissipation and thermal radiation effects are ignored,  
 71 the continuity, momentum and energy equations described the flow behavior and heat transfer

72 characteristics of natural convection within the porous cavity can be written in the following  
73 non-dimensionalized forms [16]:

74 
$$\frac{\partial u^*}{\partial x^*} + \frac{\partial v^*}{\partial y^*} = 0 \quad (2)$$

75 
$$u^* \frac{\partial u^*}{\partial x^*} + v^* \frac{\partial u^*}{\partial y^*} = -\frac{\partial p^*}{\partial x^*} - \frac{\text{Pr}_m}{\text{Da}_m} u^* + \text{Pr}_m \left( \frac{\partial^2 u^*}{\partial x^{*2}} + \frac{\partial^2 u^*}{\partial y^{*2}} \right) - \frac{1.75}{\sqrt{150}} \frac{\sqrt{u^{*2} + v^{*2}}}{\sqrt{\text{Da}_m}} u^* \quad (3)$$

76 
$$u^* \frac{\partial v^*}{\partial x^*} + v^* \frac{\partial v^*}{\partial y^*} = -\frac{\partial p^*}{\partial y^*} - \frac{\text{Pr}_m}{\text{Da}_m} v^* + \text{Pr}_m \left( \frac{\partial^2 v^*}{\partial x^{*2}} + \frac{\partial^2 v^*}{\partial y^{*2}} \right) - \frac{1.75}{\sqrt{150}} \frac{\sqrt{u^{*2} + v^{*2}}}{\sqrt{\text{Da}_m}} v^* + \text{Ra}_m \cdot \text{Pr}_m \cdot \theta \quad (4)$$

77 
$$u^* \frac{\partial \theta}{\partial x^*} + v^* \frac{\partial \theta}{\partial y^*} = \frac{\partial^2 \theta}{\partial x^{*2}} + \frac{\partial^2 \theta}{\partial y^{*2}} \quad (5)$$

78 The dimensionless boundary conditions are expressed as follows:

79 Bottom partially-heat wall:  $u^* = v^* = 0, \theta = 1$

80 Bottom other walls:  $u^* = v^* = 0, \partial \theta / \partial \bar{n}^* = 0$

81 Left and right wavy walls:  $u^* = v^* = 0, \theta = 0$

82 Top wall:  $u^* = v^* = 0, \partial \theta / \partial \bar{n}^* = 0$

83 where  $\bar{n}^*$  is the normal vector.

#### 84 2.2. Energy Flux Vectors and Nusselt Number

85 The energy flux vectors ( $\vec{E}$ ) are defined as follows [5-9]:

86 
$$\vec{E} = \frac{\partial H^*}{\partial y^*} \vec{i} - \frac{\partial H^*}{\partial x^*} \vec{j}, \quad (6)$$

87 where

88 
$$\frac{\partial H^*}{\partial y^*} = u^* \theta - \frac{\partial \theta}{\partial x^*}, \quad (7a)$$

89 
$$-\frac{\partial H^*}{\partial x^*} = v^* \theta - \frac{\partial \theta}{\partial y^*}. \quad (7b)$$

90 Note that  $H^*$  is the non-dimensional heat function, and  $\vec{i}$  and  $\vec{j}$  are the unit components  
91 in  $x$ - and  $y$ -directions, respectively.

92 The mean Nusselt number ( $Nu_m$ ) along the partially-heated bottom surface is defined as  
93 follows:

94 
$$Nu_m = \int_{0.35}^{0.65} Nud\xi, \quad (8)$$

95 where  $Nu = -\left( \frac{\partial \theta}{\partial \bar{n}^*} \right)$  is the Nusselt number.

#### 96 2.3. Geometric Description and Numerical Method

97 In this study, the left and right walls of the porous cavity are assumed to have a complex-wavy  
98 surface, which is formulated as follows [7, 8]:

99 
$$y^* = \alpha_w \sin(2\pi x^*) + \frac{\alpha_w}{2.5} \sin(4\pi x^*), \quad (9)$$

100 where  $\alpha_w$  is the wave amplitude of the wavy surface.

101 In the current study, the generalized coordinate transform technique, finite volume method  
102 and SIMPLE algorithm are used to solve the governing equations presented in Eqs. (2)~(5). The  
103 numerical methods are identical to those used in our previously studies. A detail description for the  
104 used numerical methods can be found in [7, 8].

105 *2.4. Numerical Validation and Grid Independence Evaluation*

106 The current used numerical models and numerical methods were valid by comparing the  
107 current results with those presented by Singh et al. [16]. Table 1 shows these results. Note that the  
108 Rayleigh number of  $Ra = 10^5$ , porosity of  $\varepsilon = 0.6$  and Prandtl number of  $Pr = 1$  are given in  
109 the case. It is shown that the current results are identical with those presented in Singh et al. [16].

110 The mesh sizes of  $101 \times 201$ ,  $101 \times 501$ ,  $101 \times 1001$ ,  $201 \times 1001$  have been examined for  
111 the variation of mean Nusselt number, respectively, and the results showed that the mesh size of  
112  $101 \times 1001$  has a grid-independent solution.

**Table 1.** Comparison of current results for mean Nusselt number with published results for two different Darcy numbers.

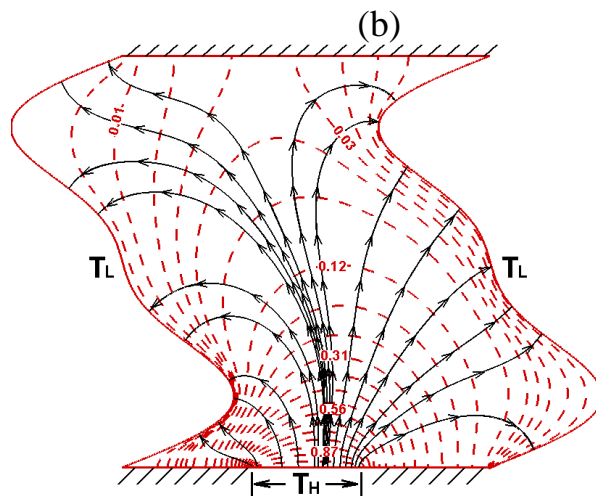
	$Da = 10^{-4}$	$Da = 10^{-2}$
Current results	3.441	1.067
Singh et al. [16]	3.461	1.067
Error (%)	0.6	0.0

113 **3. Results and discussion**

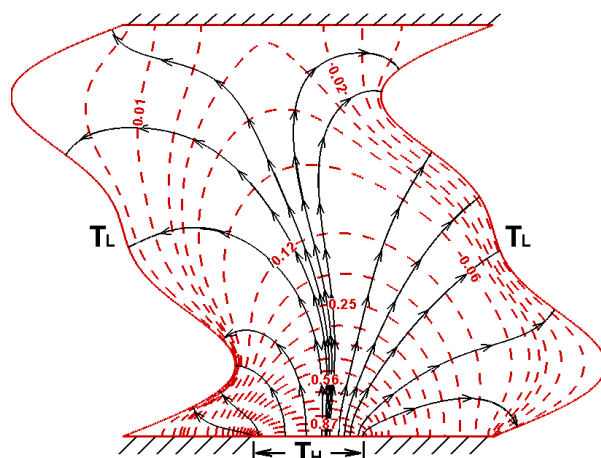
114 In the study, the wavy amplitude of the wavy surface is set to  $\alpha_w = 0.25$ , and the modified  
115 Prandtl number is given as  $Pr_m = 1.0$ .

116 Figures 2 and 3 illustrate the distributions of the energy-flux-vector within the porous cavity  
117 for various modified Darcy numbers and modified Rayleigh numbers. Figure 4 shows the effects of  
118 the modified Darcy number and modified Rayleigh number on the mean Nusselt number.  
119 According to the definition of the energy flux vectors given in Eq. (6), the conduction mechanism  
120 dominates if the flow of energy flux vectors is directly from the bottom partially-heated  
121 high-temperature wall to

122 (a)



123

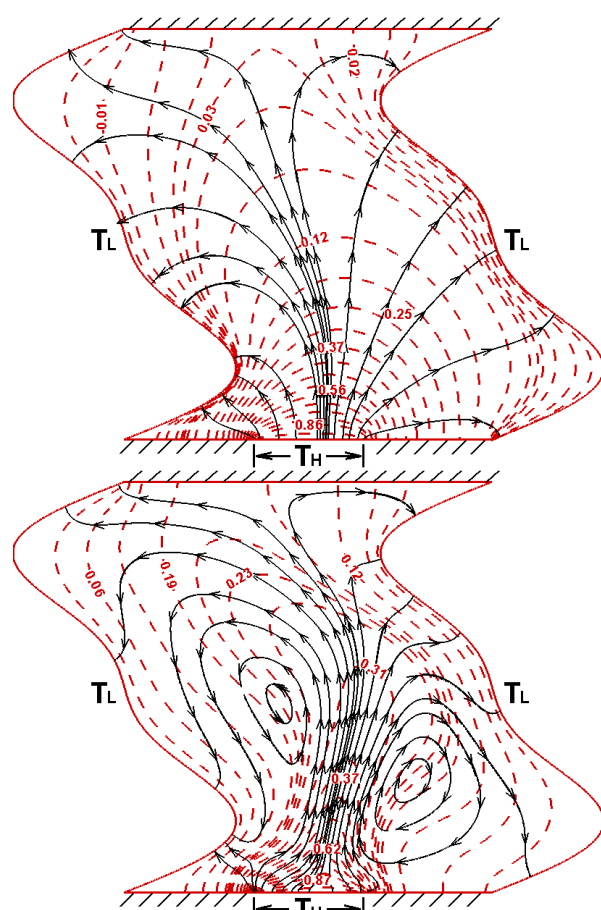


124

125 **Figure 2.** Distributions of energy flux vectors and isotherms within partially-heated porous cavity  
 126 given modified Darcy number of  $Da_m = 10^{-5}$  and modified Rayleigh number of: (a)  
 127  $Ra_m = 10^2$  and (b)  $Ra_m = 10^5$ . Note that the black solid lines indicate the flow direction of  
 128 energy-flux-vector, while the red dashed lines indicate the isothermal contours.

129 (a)

(b)



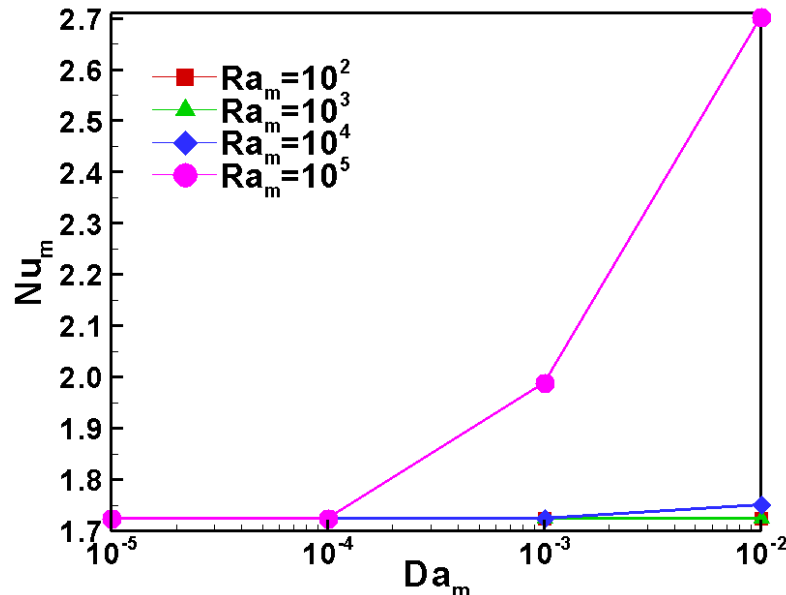
130

131

132 **Figure 3.** Distributions of energy flux vectors and isotherms within partially-heated porous cavity  
 133 given modified Darcy number of  $Da_m = 10^{-2}$  and modified Rayleigh number of: (a)  
 134  $Ra_m = 10^2$  and (b)  $Ra_m = 10^5$ . Note that the black solid lines indicate the flow direction of  
 135 energy-flux-vector, while the red dashed lines indicate the isothermal contours.

136

137



138

139  
140

**Figure 4.** Variation of mean Nusselt number with modified Darcy number as function of modified Rayleigh number.

141  
142  
143  
144  
145  
146  
147  
148  
149  
150  
151  
152  
153  
154

the left and right low-temperature wavy-walls, while the convection mechanism dominates if the energy flux vectors generate closed recirculation regions [5-9]. Therefore, as shown in Fig. 2(a), when the values of the modified Darcy number and modified Rayleigh number are both low, the heat transfer effect within the porous partially-heated cavity is dominated by a pure conduction mechanism since the closed recirculation regions in the energy-flux-vector distribution are not created. In addition, a low modified Darcy number represents a low permeability due to the present of a high flow resistance [16]. Therefore, although a larger buoyancy effect induced by giving a high modified Rayleigh number is presented, a high flow resistance is also generated within the porous partially-heated cavity. As a result, the energy flux vectors do still not form closed recirculation regions and thus conduction mechanism continually dominates heat transfer behavior (see Fig. 2(b)). Under conduction-domination, the high-temperature fluid heated by the partially-heated bottom surface is slowly diffused to left and right low-temperature wavy-wall surfaces to be dissipated. Consequently, under a low modified Darcy number, a low mean Nusselt number is presented, irrespective of the value assigned to the modified Rayleigh number (see Fig. 4).

155  
156  
157  
158  
159  
160

When a high modified Darcy number and a low modified Rayleigh number is given, the closed recirculation regions of the energy flux vectors are still not formed within the porous partially-heated cavity (see Fig. 3(a)). Although a high modified Darcy number has a high permeability and a low flow resistance, a low modified Rayleigh number induces a small buoyancy effect. Therefore, the convection effect is still weak, and the conduction mechanism continues to dominate the heat transfer effect. As a result, a low mean Nusselt number is presented (see Fig. 4).

161  
162  
163  
164  
165  
166

When the modified Darcy number and the modified Rayleigh number are both high, a low flow resistance and a high buoyancy effect occur within the porous partially-heated cavity. Therefore, the closed energy-flux-vector recirculations are formed, resulting in the domination of the convection effect (see Fig. 3(b)). The high-temperature fluid on the partially-heated bottom wall is promptly driven to the left and right low-temperature walls to be dissipated. As a result, a high mean Nusselt number is obtained (see Fig. 4).

167

#### 4. Conclusions

168  
169  
170

This paper has analyzed the heat transfer behavior of natural convection in a porous square wavy-wall cavity with a partially-heated bottom surface. To the purpose of visualization of the heat energy transport processes, the contours of energy flux vectors have been plotted. The effects of the

171 modified Rayleigh number and modified Darcy number on the energy-flux-vector distribution and  
172 mean Nusselt number have been discussed. The studied results are summarized as follows:

173 1. Given a low modified Darcy number, the energy flux vectors did not generate recirculation  
174 regions within the square porous cavity, irrespective of the value assigned to the modified  
175 Rayleigh number. The conduction mechanism dominated the heat transfer effect, and thus the  
176 mean Nusselt number was low.

177 2. Given a high modified Darcy number and a low modified Rayleigh number, the heat transfer  
178 effect was dominated by the conduction mechanism since no recirculation region was formed in  
179 the energy flux vectors. Therefore, a low mean Nusselt number was obtained.

180 3. Given a high modified Darcy number with a high modified Rayleigh number, recirculation  
181 regions in the energy-flux-vector distribution were produced, resulting in a  
182 convection-domination. Consequently, a high mean Nusselt number was presented.

183 **Acknowledgements**

184 The authors would like to thank the Ministry of Science and Technology, Taiwan, R.O.C., for  
185 the financial support of this study under Contract Nos. MOST 108-2221-E-150-011 and MOST  
186 107-2221-E-150-035.

187 **References**

- 188 1. Kimura, S.; Bejan, A. The "Heatline" visualization of convective heat transfer. *J. Heat Transf.-Trans. ASME*  
189 **1983**, *105*, 916-919.
- 190 2. Trevisan, O.V.; Bejan, A. Combined heat and mass transfer by natural convection in a vertical enclosure. *J.*  
191 *Heat Transf.-Trans. ASME* **1984**, *109*, 104-112.
- 192 3. Ramakrishna, D.; Basak, T.; Roy, S.; Pop, I. A complete heatline analysis on mixed convection within a  
193 square cavity: Effects of thermal boundary conditions via thermal aspect ratio. *Int. J. Therm. Sci.* **2012**, *57*,  
194 98-111.
- 195 4. Biswal, P.; Nag, A.; Basak, T. Analysis of thermal management during natural convection within porous  
196 tilted square cavities via heatline and entropy generation. *Int. J. Mech. Sci.* **2016**, *115-116*, 596-615.
- 197 5. Hooman, K.; Gurgenci, H. Dincer, I., Heatline and energy-flux-vector visualization of natural convection  
198 in a porous cavity occupied by a fluid with temperature-dependent viscosity. *J. Porous Media* **2009**, *12*,  
199 265-275.
- 200 6. Hooman, H. Energy flux vectors as a new tool for convection visualization. *Int. J. Numer. Methods Heat*  
201 *Fluid Flow* **2010**, *20*, 240-249.
- 202 7. Cho, C.C. Heat transfer and entropy generation of mixed convection flow in Cu-water nanofluid-filled  
203 lid-driven cavity with wavy surface. *Int. J. Heat Mass Transf.* **2018**, *119*, 163-174.
- 204 8. Cho, C.C. Mixed convection heat transfer and entropy generation of Cu-water nanofluid in wavy-wall  
205 lid-driven cavity in presence of inclined magnetic field. *Int. J. Mech. Sci.* **2019**, *151*, 703-714.
- 206 9. Nayak, R.K.; Bhattacharyya, S. Pop, I., Numerical study on mixed convection and entropy generation of a  
207 nanofluid in a lid-driven square enclosure. *J. Heat Transf.-Trans. ASME* **2016**, *138*, 012503.
- 208 10. Nield, D.A.; Bejan, A. *Convection in Porous Media*, New York: Springer-Verlag, 2006.
- 209 11. Al-Amiri, A.; Khanafer, K.; Pop, I. Steady-state conjugate natural convection in a fluid-saturated porous  
210 cavity. *Int. J. Heat Mass Transf.* **2008**, *51*, 4260-4275.
- 211 12. Kumar, B.V.R.; Singh, P.; Murthy, P.V.S.N. Effect of surface undulations on natural convection in a porous  
212 square cavity. *J. Heat Transf.-Trans. ASME* **1997**, *119*, 848-851.
- 213 13. Chen, X.B.; Yu, P.; Winoto, S.H.; Low, H.T. Free convection in a porous wavy cavity based on the  
214 Darcy-Brinkman-Forchheimer extended model. *Numer. Heat Transf. A-Appl.* **2007**, *52*, 377-397.
- 215 14. Khanafer, K.; Al-Azmi, B.; Marafie, A.; Pop, I. Non-Darcian effects on natural convection heat transfer in a  
216 wavy porous enclosure. *Int. J. Heat Mass Transf.* **2009**, *52*, 1887-1896.
- 217 15. Biswal, P.; Basak, T. Heatlines visualization of convective heat flow during differential heating of porous  
218 enclosures with concave/convex side walls. *Int. J. Numer. Methods Heat Fluid Flow* **2018**, *28*, 1506-1538.
- 219 16. Singh, A.K.; Basak, T.; Nag, A.; Roy, S. Heatlines and thermal management analysis for natural convection  
220 within inclined porous square cavities. *Int. J. Heat Mass Transf.* **2015**, *87*, 583-597.

